From molecular clusters to bulk matter. I. Structure and thermodynamics of small CO2, N2, and SF6 clusters

Article *in* The Journal of Chemical Physics · July 1998

DOI: 10.1063/1.476509

5 authors, including:

Florent Calvo
Joseph Fourier University
297 PUBLICATIONS **7,293** CITATIONS

SEE PROFILE

From molecular clusters to bulk matter. I. Structure and thermodynamics of small CO_2, N_2, and SF_6 clusters

Jean-Bernard Maillet, Anne Boutin, and Séverine Buttefey
Laboratoire de Chimie-Physique des Matériaux Amorphes, Department of Physical Chemistry, Bâtiment 490, Université Paris-Sud, 91405 Orsay, France

Florent Calvo
Laboratoire Collisions, Agrégats, Réactivité, IRSAMC, Université Paul Sabatier, 118 Route de Narbonne, 31062 Toulouse, France

Alain H. Fuchs[a)]
Laboratoire de Chimie-Physique des Matériaux Amorphes, Department of Physical Chemistry, Bâtiment 490, Université Paris-Sud, 91405 Orsay, France

(Received 6 August 1997; accepted 23 March 1998)

The thermodynamics and structural properties of small molecular X_N clusters ($X=N_2$, CO_2, and SF_6) are investigated using molecular dynamics simulations. In this paper we compare the behavior of carbon dioxide, nitrogen, and sulfur hexafluoride for a given cluster size of $N=13$. Evidence is provided for ''dynamical coexistence'' between solidlike and liquidlike forms of the cluster, in a finite energy range, in the case of $(CO_2)_{13}$ and $(N_2)_{13}$ but not $(SF_6)_{13}$. In addition $(N_2)_{13}$ exibits a solid–solid phase transition characterized by the release of the molecular orientational degree of freedom. A systematic use of the dynamic quenching method enables us to interpret these different behaviors in terms of the energy distribution of minima in the potential energy surface of the systems. A comparison of the strain energies of these clusters, using a model recently proposed by Wales and co-workers, enables us to understand why different molecular clusters exhibit different crossover points from icosahedral to bulk properties. © *1998 American Institute of Physics.* [S0021-9606(98)00425-5]

I. INTRODUCTION

Clusters often exhibit unique properties which are different from both the properties of the individual atom or molecule and from those of the bulk matter. For instance low energy solidlike structures with icosahedral symmetry are observed in small van der Waals or metal clusters. The crossover to the crystalline bulklike structure occurs in a size range which depends upon the type of system. In the case of van der Waals systems, small rare gas clusters have polyicosahedral then multishell icosahedral structures which persist up to sizes $N\approx 1000-2000$ atoms.[1,2] On the other hand, experiments and computer simulations have shown that clusters of small quasispherical molecules such as CCl_4 exhibit a crystalline packing arrangement when they contain as few as $\sim$100 molecules.[3] An estimate of the onset of crystalline behavior for nitrogen is a few hundred molecules.[4] For SF_6 clusters, the crossover from noncrystalline to crystalline bulklike structure occurs in the size range of 13–19 molecules[5,6] and for CO_2 clusters in the range of 25–32 molecules.[7] Recently, Scoles and co-workers[8] have suggested that the favored structure of small cyanoacetylene clusters switches at $N=4$ from a cyclic to a stacked arrangement which bears some resemblance to the crystal structure. This dramatic difference in behavior between atomic and polyatomic systems has been attributed to the anisotropy of the repulsive part of the intermolecular potential,[4,6] but it is still not fully understood.

Irregular size dependencies were observed by computer simulations in the structural and thermodynamic properties of small Lennard-Jones (LJ) clusters, in the size range of ten to a few hundred atoms.[9,10] This is related to the fact that certain ''magic numbers'' of identical atoms may form compact icosahedral structures. In addition $(LJ)_N$ clusters of several sizes ($N=7,11,13,19,55,...$) were shown to display a melting phase transition apparently quite unlike the bulk one. Instead of showing two phases coexisting in contact, a ''dynamical coexistence'' phenomenon was found, in a finite range of energy, between solidlike and liquidlike forms of the clusters.[11,36] Melting with dynamical coexistence has also been found in polyatomic systems such as $(H_2O)_8$ and $(H_2O)_{20}$ (Ref. 12) and recently in $(N_2)_{13}$,[13] but not in $(SF_6)_N$ clusters, $N=7-55$.[5]

Many aspects of the thermodynamics of clusters are still not well understood. For instance, the mechanism of the icosahedral to crystalline transformation, as the number of molecules increases, is unknown.[14] Also, some questions regarding the coexistence melting phenomenon remain open, although it has been well characterized in LJ systems.[15,16] Several theoretical studies have shown that it should be understood as the microscopic finite size system analog of the bulk first-order melting transition.[8,17–20] Thus the dynamical coexistence must, at some stage, turn into a static coexist-

a)Author to whom correspondence should be addressed, electronic mail: fuchs@cpma.u-psud.fr

TABLE I. Lennard-Jones parameters of the potential function for CO_2 and location of the five partial charges of the molecule (Ref. 23). z represents the coordinate along the molecule axis, the origin is the carbon atom. The C–O bond length is 1.16 Å.

Lennard-Jones parameters	ϵ (K)	σ (Å)
C–C	26.3	2.824
O–O	75.2	3.026
Partial charges	z (Å)	$q(\|e\|)$
1	−1.5232	0.1216
2	−1.0663	−0.6418
3	0	−1.0404
4	1.0663	−0.6418
5	1.5232	0.1216

TABLE II. Buckingham parameters of the potential function ($Ae^{-\alpha r} - (C_6/r^6)$) for N_2 and location of the four partial charges of the molecule (Ref. 25). z represents the coordinate along the molecule axis, the origin is the molecule center of mass. The N–N bond length is 1.094 Å.

Buckingham parameters	α(Å^{-1})	A (kJ/mol)	$C6$(kJ/mol)
	3.461 136	125 502.7	1641.2749
Partial charges	z (Å)	$q(\|e\|)$	
1	−1.044	−0.373	
2	−0.847	+0.373	
3	0.847	+0.373	
4	1.044	−0.373	

ence as N increases. Not much is known about the mechanism of this transformation.[14] It is also unclear whether or not the transformations mentioned above (the icosahedral to crystalline and the dynamical to static coexistence melting processes) take place in the same cluster size range (i.e., to what extent are these phenomena coupled together?).

In order to address these points we have undertaken a molecular dynamics study of small molecular clusters. Following Wales and co-workers[10–12,15,21,22] we characterize the structural, dynamic, and thermodynamic changes in terms of the underlying potential energy surface (PES) of the system. Understanding the thermodynamic properties of a given cluster requires a knowledge of the PES minima. It is also necessary to consider local minima on the PES other than the lowest, because these may be populated at finite temperatures.

In this paper we compare the behaviors of different systems, namely carbon dioxide, nitrogen, and sulfur hexafluoride for a given cluster size of $N=13$. We examine the structures and the melting process and relate the observed behavior to the energy distribution of the minima in the PES. A comparison of the strain energies of these clusters, using a model recently proposed by Wales and co-workers[21,22] enables us to understand the difference in crossover point from icosahedral to bulk properties between these systems.

II. SIMULATION DETAILS

Molecular dynamics (MD) simulations were performed using effective two-body atom–atom intermolecular potentials. For carbon dioxide clusters we have used the one proposed[23] for bulk CO_2 and used in previous clusters simulations.[7,24] It consists of an electrostatic interaction term produced by five collinear partial charges located on the symmetry axis of each molecule, plus a term of the (6–12) Lennard-Jones form. The ten parameters of the potential function are given in Table I. Similarly, the nitrogen intermolecular potential proposed for bulk N_2 was used.[25] It consists of four partial charges located on the N–N bond plus a term of the Buckingham form. The parameters for this potential are given in Table II. The intermolecular potential for sulfur hexafluoride is a simple LJ atom–atom potential with no Coulombic term. It has been described in detail in earlier works.[5] The parameters of these potentials were fitted to reproduce the bulk properties. No boundary conditions were used in the simulations. The molecules were considered as rigid bodies.

Both microcanonical and canonical trajectories were generated, the latter by using the Nosé thermostat algorithm.[26] The average temperature obtained with this algorithm is within a 0.001% error. The characteristic time of the temperature fluctuations of the system and the heat exchange frequency have been compared in order to test the efficiency of the thermal coupling between the thermostat and the cluster. The coupling is assumed to be effective when these two times are of the same order of magnitude. The chosen value of the coupling parameter Q was 10 kJ mol^{-1} ps. Both translational (coordinates of the centers of mass) and orientational (quaternions) degrees of freedom were coupled to the Nosé thermostat. The results obtained by canonical MD simulations have been compared with those of canonical Monte Carlo (MC) simulations (Davis *et al.* have shown that equilibrium and some dynamical properties are independent of the value of the Q parameter[27]). The position and quaternion coordinates were time-stepped using the Beeman algorithm.[28] This time-step algorithm is accurate to the same level of approximation as the more commonly used Verlet algorithm for position, but also for velocity integration step. This is very useful when using a thermostat algorithm in a canonical simulation. A time step of 5.0 fs was used. At a given temperature, equilibration runs of ~200 ps runs were performed, followed by 500 ps to 10 ns production runs performed in both the canonical and microcanonical ensembles.

MC simulations have been performed using the same intermolecular potentials as in molecular dynamics. The cluster orientation was kept constant during the simulation, in order to calculate the orientational order parameter defined below. This is done by using an Eckart-type constraint for the random MC displacement $\delta\mathbf{r_i}$ of the positions $\mathbf{r}_i$:

$$\sum_{i=1}^{N} m_i \mathbf{r}_i \times \delta\mathbf{r}_i = \mathbf{0}. \tag{1}$$

MD runs were performed at different temperature and energy values, from which the stable minima of the potential energy surface (PES) were searched by using the dynamic quenching method (DQM). DQM is similar in nature to the steepest descent method, which was first used in molecular dynamics by Stillinger *et al.*[29,30] and enables one to find

minimum energy configurations starting from a dynamical trajectory. It consists in applying a frictional damping factor on both force and torque terms in the equations of motion of each molecule.[31,32] The new equation of motion becomes

$$\ddot{\mathbf{r}}_i = -\nabla\phi - k\dot{\mathbf{r}}_i. \tag{2}$$

Starting from a configuration in the classical trajectory, the system is gradually cooled down to a minimum. During its evolution the system can probe different minima of the PES. DQM was chosen rather than the more commonly used conjugate gradient technique because we were using a (transputer-based) parallel computer in which a molecular dynamics algorithm can be more efficiently implemented. Moreover, the advantage of the DQM over the steepest descent or the conjugate gradient technique, is that the probability of finding a particular minimum depends not only on its width but also on its depth. When the system flies over a deep well, its kinetic energy is high and so is the friction factor. Thus a narrow and deep well will have a larger appearance frequency using the DQM method. The total quenching time in DQM, i.e., the time needed to reach a temperature arbitrarily fixed to 10^{-8} K is monitored by the value of the damping parameter k. Tests showed that this time is minimal for k values between 2 and 5 ps^{-1}, whatever the initial temperature was. In this work the value of $k = 2\ ps^{-1}$ was used. Between 1000 and 3000 MD quenches were made for each cluster.

We have assigned a temperature to each of the studied rotationless and translationless clusters. This corresponds to the average kinetic temperature calculated using the equipartition theorem

$$T = \frac{2\langle E_K\rangle}{(5N-6)k_B}, \tag{3}$$

where $\langle E_K\rangle$ is the mean kinetic energy of the cluster and k_B is the Boltzmann constant.

In order to characterize the state of the cluster at a given temperature, we have used Lindemann's δ defined as:

$$\delta = \frac{2}{N(N-1)} \sum_{i<j}^{N} \frac{(\langle r_{ij}^2\rangle_t - \langle r_{ij}\rangle_t^2)^{1/2}}{\langle r_{ij}\rangle_t}, \tag{4}$$

where r_{ij} is the distance between molecular centers of mass.

In the case of nitrogen and carbon dioxide clusters we have computed an orientational order parameter:

$$\langle \cos\ \theta\rangle = \left| \left\langle \frac{1}{N} \sum_i \cos\ \theta_i(t) \right\rangle \right|, \tag{5}$$

where θ_i is the angle between the molecular axis of a molecule at time t and its corresponding orientation in the global minimum.

The heat capacity $C_v(T)$ of a cluster was calculated in both canonical Nosé dynamics using total energy fluctuations,

$$C_v = \frac{\langle E_t^2\rangle - \langle E_t\rangle^2}{kT^2}. \tag{6}$$

In canonical MC simulations, the multiple histogram method was used to calculate the heat capacity.[17]

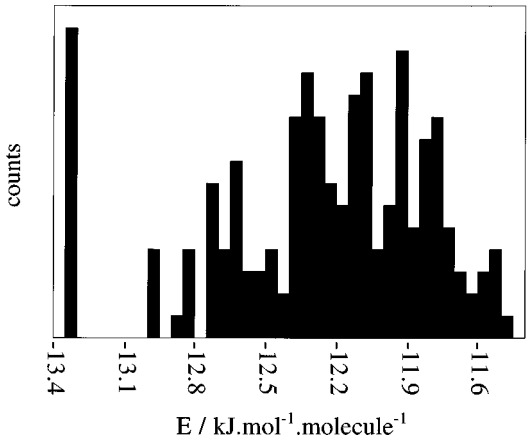

FIG. 1. Energy distribution of the PES minima of the $(CO_2)_{13}$ cluster obtained from ~1000 MD quenches.

III. RESULTS

A. Structure and thermodynamics of the $(CO_2)_{13}$ cluster

Canonical and microcanonical MD runs have been performed on the $(CO_2)_{13}$ cluster. An initial configuration was created in a cubic bulklike structure. The fcc structure turned out to be unstable and an instantaneous rearrangement from cubic to icosahedral structure took place in the first picosecond of the simulation at 10 K. The system was then gradually heated up to 110 K, above its melting point (no evaporation took place during the course of these relatively short runs), and then cooled down, back to the initial temperature using canonical simulations. No hysteresis was found in the caloric curve.

Quenches have been performed starting from roughly 1000 configurations picked up every 5 ps along a trajectory at 100 K in the liquid state. The energy distribution of the PES minima is shown in Fig. 1. The global minimum is found at a potential energy of $-13.3408\ kJ\ mol^{-1}$ per molecule. The point group is $3(i, C_3, C_3^2, S_6, S_6^5)$, and the molecular centers of mass form a regular icosahedron (Fig. 2).

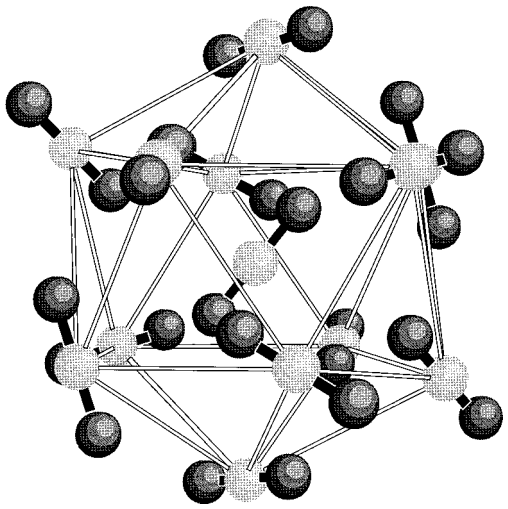

FIG. 2. The structure of the global minimum in the PES for $(CO_2)_{13}$.

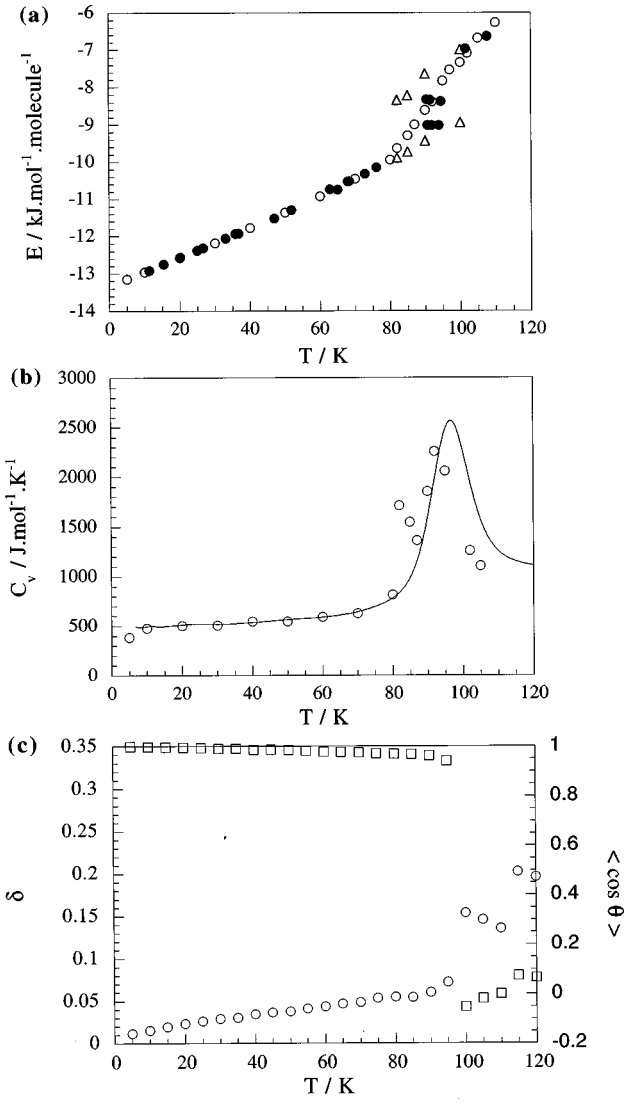

FIG. 3. Thermodynamics of the $(CO_2)_{13}$ cluster: Open and full symbols correspond to canonical and microcanonical runs, respectively. (a) The caloric curve calculated from MD simulations. Circles correspond to long time averages. Triangles correspond to the stable solidlike and liquidlike forms between which the dynamical coexistence phenomenom is observed. The broken line is a guide to the eye. (b) Molar heat capacity computed from the energy fluctuations in the canonical MD runs. The solid line is the MC heat capacity curve calculated from the multiple histogram method. (c) Squares: the orientational order parameter ($\langle \cos \theta \rangle$) as a function of temperature. Circles: the translational (relative root-mean-square intermolecular separation, δ) order parameter as a function of temperature. Both parameters were calculated using MC simulations.

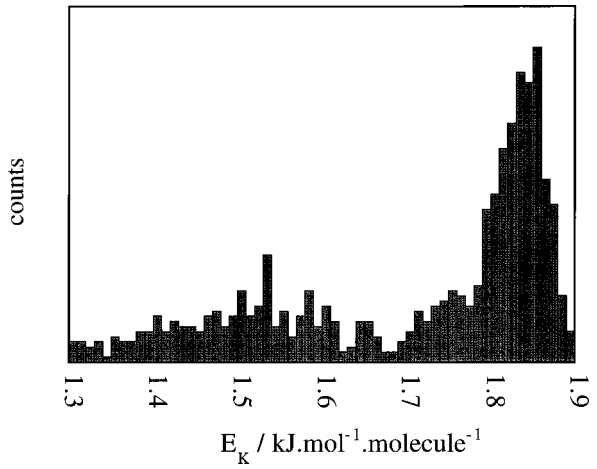

FIG. 4. Distribution of short-time-averaged internal kinetic energy during a 4 ns microcanonical run at a total energy of $-9.02\ \mathrm{kJ\ mol^{-1}\ molecule^{-1}}$ using a period of 1000 steps.

The alternative notation for this point group is S_6. An energy gap is observed in the energy distribution of the PES minima. Some of the higher energy local minima are always icosahedral (slightly distorted) from the point of view of the centers of mass but are orientationaly disordered. The others local minima correspond to loosely bound (amorphous) structures. These latter minima are associated with the liquid state.

The caloric curve $E(T)$ and the corresponding molar heat capacity, calculated from energy fluctuations in the canonical runs, are shown in Fig. 3. Both curves indicate the melting event at $T \approx 95$ K. The heat capacity curves calculated by canonical Nosé dynamics and Monte Carlo simulations are compared in Fig. 3(b). At very low temperature (below ~4 K) the heat capacities have not been reported because the small fluctuations of the total energy of the cluster lead to a very large uncertainty. At high temperature (above melting) good statistics cannot be obtained because of the occurrence of evaporation events (MD runs were stopped after each evaporation event). In MC simulations we have used a repulsive wall located at 10 Å from the cluster center of mass (9 Å in the case of nitrogen clusters). This procedure allows us to deal with the evaporation problems but it also induces some kind of confinement effects in the thermodynamic properties. This presumably explains the small differences in the heat capacity curves at high temperature. However, there is an overall good agreement between the results of MD and MC simulations in the main temperature range of interest, from ~5 to ~95 K. This is satisfactory and confirms a previous work on LJ systems.[33]

A bimodal distribution is observed, in a finite range of energy corresponding to melting, in the probability distribution of the short-time averaged internal kinetic energy of the system in the microcanonical ensemble (Fig. 4). A bimodal distribution of the *total* energy is also observed in the canonical simulations. The maxima in these distribution functions are plotted in Fig. 3(a) (triangles). Coexistence is observed between the solidlike and liquidlike forms (in much the same way as in LJ_{13}).[10] The coexisting states correspond to *liquidlike* and *solidlike structures*, respectively. Following Bixton and Jortner[34] and Berry and Wales,[10] the dynamical coexistence phenomenon is tentatively associated with the existence of an energy gap between the *solid* and *liquidlike minima* in the PES. At low energy the cluster is trapped in the *solidlike local minimum*. In the intermediate energy range, the system begins to visit the higher potential energy minima. It jumps back and forth from the global (icosahedral) minimum to the distribution of loosely bound high energy structures which correspond to the liquid state. This process corresponds to the dynamical coexistence phenomenon.[35] At sufficiently higher energy, the system is in the liquidlike state: it mainly explores the distribution of high potential energy amorphous minima.[36] In the microcanonical

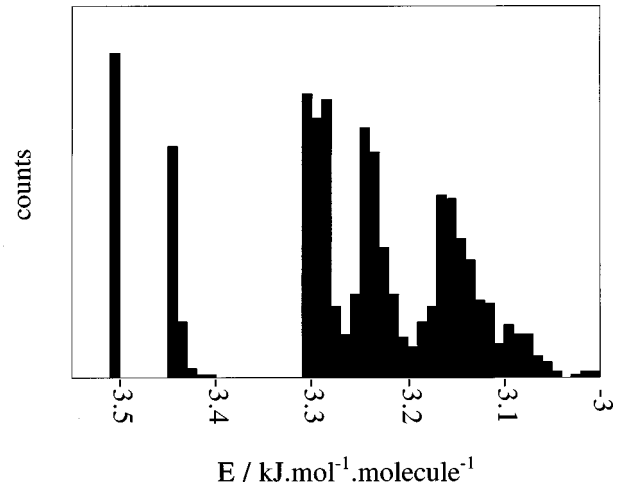

FIG. 5. Energy distribution of the PES minima of the $(N_2)_{13}$ cluster obtained from ~3000 MD quenches.

caloric curve, melting is characterized by a more abrupt change in the slope of $E(T)$, and it takes place in a narrower temperature range than in the canonical ensemble. Still the microcanonical caloric curve exhibits an inflexion rather than the expected *S* bend, for reasons that are presumably similar to the $(LJ)_{13}$ case.[10,11,37]

Figure 3(c) displays the computed change in translational (Lindemann's δ) and orientational $\langle \cos\theta \rangle$ order parameters with temperature for $(CO_2)_{13}$. Clearly the translational and orientational degrees of freedom are both released at $T \approx 95$ K.

Etters *et al.*[38] have observed in Monte Carlo simulations some changes in the energy and orientational order of very small CO_2 clusters ($N=2-13$) as a function of temperature. These were attributed to the existence of an orientational phase transition. However, this early attempt was handicapped by the lack of statistical mechanics tools that nowadays enable one to explain structural, dynamics, and thermodynamics changes in terms of the underlying potential energy surface of the system under investigation.[22] We believe that Etters *et al.*[38] did not find the global minimum in their MC simulations of $(CO_2)_{13}$ although there are some slight differences between the potentials used by these authors and the one used in the present study. Their lowest-energy cluster was found at -12.43 kJ mol^{-1} per molecule and is described as a distorted icosahedron. The phenomenon observed by these authors is presumably due to a spontaneous irreversible transition from the initially distorted icosahedral cluster (which is presumably a local minimum in the PES) to the regular icosahedron which corresponds to the global minimum in the PES. An independent investigation of the thermodynamics of $(CO_2)_{13}$ through Monte Carlo and Nosé dynamics by Weerasinghe and Amar[31] did not show any sign of low temperature orientational phase transition.

B. Structure and thermodynamics of the $(N_2)_{13}$ cluster

Figure 5 displays the energy distribution of the PES minima of the $(N_2)_{13}$ cluster. A similar energy distribution was recently found by Bertolus *et al.* using a Monte Carlo growth technique.[32] This presumably indicates that most of the significant local minima on the PES were found by our MD quenches. The most prominent feature of this distribution is the observation of three sets of local minima separated by two energy gaps. The first set corresponds to two isomers: the global minimum is found at a potential energy of -3.5034 kJ mol^{-1} per molecule and another low lying minimum is observed at -3.5004 kJ mol^{-1} per molecule. Both minima belong to the class of icosahedral packing. The point group of the global minimum is $\bar{3}$ as in the case of $(CO_2)_{13}$ and the molecular centers of mass form a regular icosahedron. The other low lying minimum has a similar but slightly distorted structure. In the energy range between -3.4480 and -3.4098 kJ mol^{-1} per molecule a second set is found which contains five local minima. All five isomers are icosahedral (more or less distorted) from the point of view of the centers of mass, but now the molecules exhibit uncorrelated orientations, so that the central molecule is no longer a center of symmetry of the cluster. As the total energy is increased the quenches find higher lying minima. This corresponds to the third set of local minima which is found above an energy of -3.3066 kJ mol^{-1} per molecule. All these minima correspond to loosely bound (amorphous) structures, some of them being close to defective icosahedrons.

Canonical and microcanonical MD runs have been performed in the temperature range $0\,K < T < 36$ K, starting from the global minimum found on the PES, in order to investigate the thermodynamic behavior of the $(N_2)_{13}$ cluster. The caloric curve and the corresponding molar heat capacity, calculated from energy fluctuations in the canonical runs, are shown in Figs. 6(a) and 6(b). The heat capacity calculated from MC simulations is also plotted in Fig. 6(b). As in the $(CO_2)_{13}$ cluster, a good agreement is observed between canonical MD and MC simulations. Both the caloric and the heat capacity curves indicate the melting event at $T \approx 30$ K. A coexistence is again observed between the solidlike and liquidlike forms. In the present case, melting can be associated with the larger energy gap between the second and the third set of local minima found in the PES (Fig. 5).

We shall now focus on the smaller and broader peak observed at low temperature in the heat capacity curve. As shown in Fig. 6(c), there is clearly a gradual loss of orientational order of the molecules from the lowest temperature up to ~10 K. The loss of orientational correlation is obviously slow so that the resulting heat capacity peak is broad and the change in slope of the caloric curve can hardly be observed. This transition may be associated with the small energy gap between the *rigid solidlike minima* and the *rigid orientationally disordered minima* in the PES (the gap between the first and second set of local minima seen in Fig. 5). Also shown in Fig. 6 is Lindemann's δ as a function of temperature, indicating that the translational melting process is initiated at $T \approx 25$ K (refering to Lindemann's melting criteria of $\delta \sim 0.1$).

Clearly, the heat capacity peak observed at $T \approx 10$ K in the $(N_2)_{13}$ cluster can be attributed to the release of the molecular orientational degree of freedom. This peak is also observed in larger magic number clusters such as $(N_2)_{55}$. Its

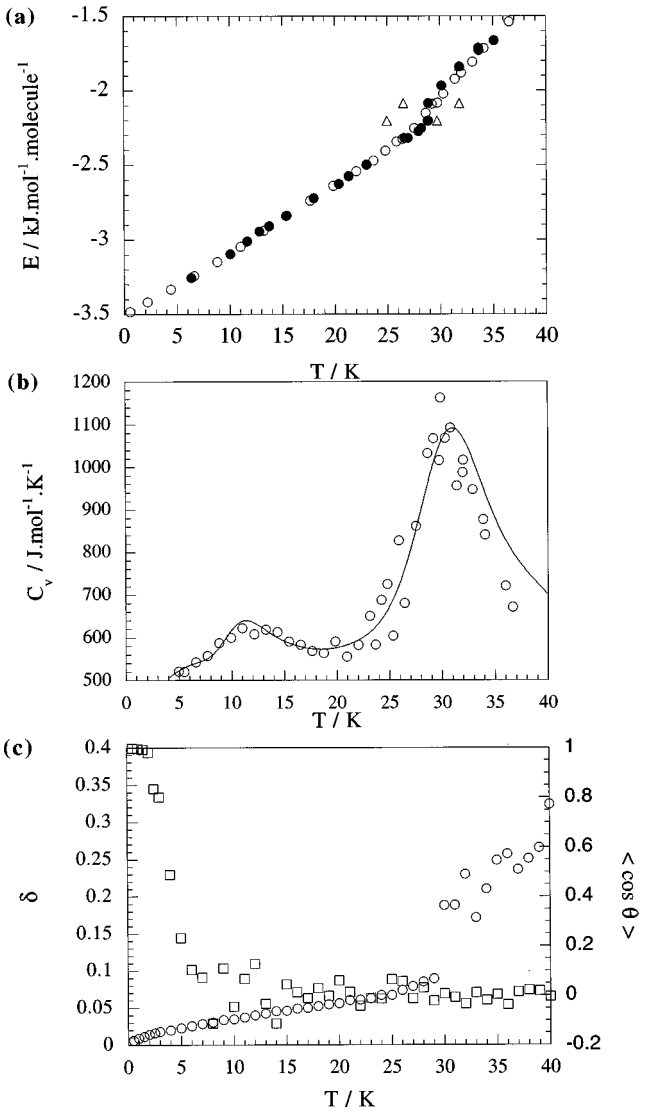

FIG. 6. Thermodynamics of the $(N_2)_{13}$ cluster: Open and full symbols correspond to canonical and microcanonical runs, respectively. (a) The caloric curve calculated from MD simulations. Circles correspond to long time averages. Triangles correspond to the stable solidlike and liquidlike forms between which the dynamical coexistence phenomenon is observed. The broken line is a guide to the eye. (b) Molar heat capacity computed from the energy fluctuations in the canonical MD runs. The solid line is the MC heat capacity curve calculated from the multiple histogram method. (c) Squares: the orientational order parameter ($\langle\cos\theta\rangle$) as a function of temperature. Circles: the translational order parameter (relative root-mean-square intermolecular separation, δ) as a function of temperature. Both parameters were calculated using MC simulations.

bulk phase counterpart could well be the rotational phase transition from a rigid to a plastic crystal which is known to occur[39] in solid N_2. The transition observed in the present study is thus presumably a finite size system analog of a bulk solid–solid phase transition.

C. Structure and thermodynamics of the $(SF_6)_{13}$ cluster

This model cluster has already been investigated in some detail in an earlier work.[5] We have shown that $(SF_6)_{13}$ displays a featureless caloric curve and a unimodal short-time

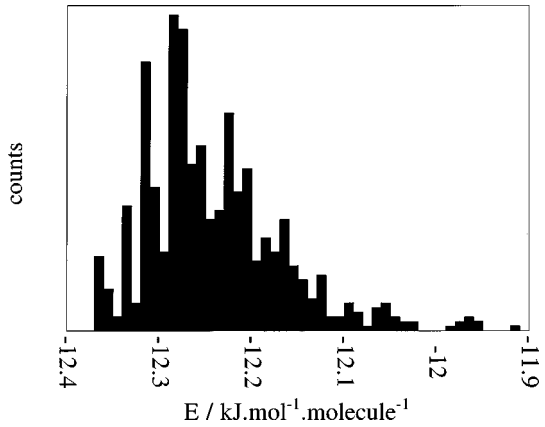

FIG. 7. Energy distribution of the PES minima of the $(SF_6)_{13}$ cluster obtained from ~1500 MD quenches.

averaged kinetic energy distribution for all energies. The global minimum is amorphous and the centers of mass form a highly distorted icosahedron. In addition to this previous study, the energy distribution of the PES minima was computed (Fig. 7). A broad distribution of low energy minima corresponding to quasidegenerate rearrangements of the distorted icosahedron is observed in the PES. No energy gap is observed in the PES and this presumably explains why coexistence has not been observed in this case.

IV. DISCUSSION

A. Phase transitions in small molecular clusters

Phase transitions have been observed in model systems in the regime of small molecular clusters, in Jortner's terms.[40] In the case of the melting transition, coexistence has been observed for model $(CO_2)_{13}$ and $(N_2)_{13}$. It is characterized by a bimodal distribution in the probability distribution of the short-time averaged kinetic energy of the system. This is interpreted in terms of the energy distribution of the PES minima. Clusters for which an energy gap exists between the low energy *solidlike minima* and the distribution of high energy minima associated with the liquidlike state may experience a dynamical coexistence (provided that the energy barrier between the solidlike and liquidlike states is not too high). In the small size regime, the occurrence of dynamical coexistence may clearly depend on the exact number of molecules in the cluster. Clusters which form one (or a few) compact stable solidlike structures at low temperature are likely to exhibit dynamical coexistence. This will depend on the geometry and force field of the system. Coexistence has been observed in the cases of $(LJ)_{13}$ (Ref. 11) and $(CO_2)_{13}$ for which a single global minimum was found [icosahedron I_h in the case of $(LJ)_{13}$ and $\bar{3}$ point group with the molecular centers of mass forming a regular icosahedron in the cases of $(CO_2)_{13}$]. In addition to the $\bar{3}$ global minimum, $(N_2)_{13}$ displays a set of five low lying local minima. They correspond to icosahedron from the point of view of the centers of mass, but now the molecules exhibit uncorrelated orientations, so that the central molecule is no longer a center of symmetry of the cluster. This set of local minima is separated from the liquidlike minima by an energy gap, so

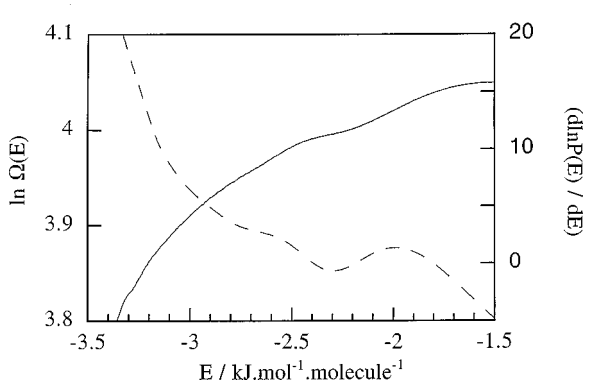

FIG. 8. Logarithm of the density of states of the $(N_2)_{13}$ cluster plotted against E and the derivative of the logarithm of the probability distribution function (dotted curve) at $T=30$ K calculated using the multiple histogram method. The density of states is correct to within an unknown multiplicative factor. The bimodality observed in $d \ln P(E)/dE$ corresponds to a van der Waals loop in the microcanonical caloric curve.

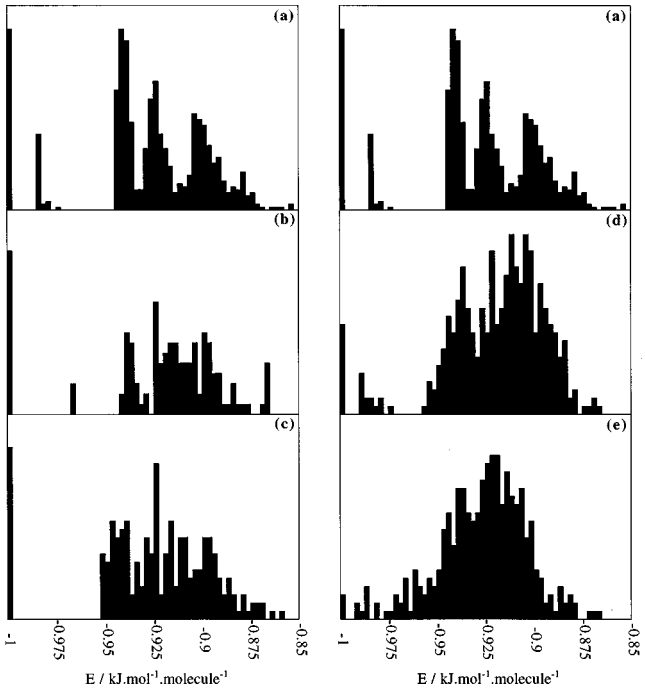

FIG. 9. Normalized energy distribution of the PES minima of several $(X)_{13}$ model clusters in which we have arbitrarily increased the molecular quadrupole moment or the internuclear separation: (a) nitrogen; (b) nitrogen with $(1.5)Q_{N_2}$; (c) nitrogen with $2Q_{N_2}$; (d) nitrogen with $(1.5)l_{N_2}$; (e) nitrogen with $2l_{N_2}$.

that coexistence is also observed in $(N_2)_{13}$. On the other hand $(SF_6)_{13}$ displayed a broad distribution of low energy minima in the PES corresponding to quasidegenerate rearrangements of the distorted icosahedron, and this can be correlated with the absence of coexistence in this system.

Coexistence was not always observed in LJ clusters. For instance, $(LJ)_{8,14}$ did not show coexistence while $(LJ)_{7,13}$ did.[9,11,16] Nonmagic number clusters may however exhibit coexistence, provided that the number of low-lying minima is not too high and that they are separated from the liquidlike minima by an energy gap. This was found in $LJ_{11,15}$. In a recent study of $(CO_2)_{12,14}$ we have observed in both cases the coexistence phenomenon and a gap in energy between the low lying wells and the distribution of liquidlike high energy minima in the PES.[35] Thus, the correlation between dynamical coexistence and the occurrence of an energy gap in the PES seems to be confirmed.

In addition we have also shown the possible occurrence of an orientational transition in small clusters, which is also correlated with an energy gap in the PES. The fact that this transition has been observed in model $(N_2)_{13}$ and $(N_2)_{55}$ but not in $(CO_2)_{13}$ seems to indicate that it is the finite size analog of the bulk rigid to plastic phase transition, which is known to occur in solid N_2 but not in CO_2. We have tried to find out whether or not this orientational transition is associated with a dynamical coexistence phenomenon, just like the melting transition. Coexistence is associated with the observation of two inflections in the logarithm of the density of states $[\ln \Omega(E)]$ and it should be stressed once again that it can be different from the ''coexistence'' deduced from short time averages.[11,17] As shown in Fig. 8, this is clearly observed for the melting transition in $(N_2)_{13}$ in the vicinity of $E=-2.2$ kJ mol^{-1} molecule^{-1}. The two associated local extrema in the derivative of $\ln P(E)$ versus energy define an energy interval in which coexistence in the microcanonical ensemble is observed. No such behavior is observed in the vicinity of $E=-3$ kJ mol^{-1} molecule^{-1}. Thus it seems that the orientational transition is not associated with a coexistence phenomenon.

The occurrence of an orientational transition is crucially dependent on the intermolecular force field. We have investigated the PES for a model $(N_2)_{13}$ in which we have arbitrarily modified the values of the partial charges (thus modifying the quadrupole moment), or of the internuclear distance. As shown in Fig. 9, the double gap observed in $(N_2)_{13}$ tends to disappear when either the quadrupole moment or the internuclear distance is increased. Increasing the quadrupole moment results in a shifting of the orientationally disordered minima to higher energy, and increasing the internuclear distance results in a shifting of the liquidlike minima to lower energy. Since both the quadrupole moment and internuclear distance are larger in CO_2 than in N_2, this explains why a single gap (and no orientational transition) was observed in $(CO_2)_{13}$.

B. How small is a molecular crystal?

We now turn into another type of comparison between X_{13} clusters (X=Ar, CO_2, N_2, SF_6), in order to shed some light on the difference in behavior between atomic and polyatomic systems mentioned in the introduction of this paper.

For this we use a model recently proposed by Wales and co-workers.[21,22] In this model, the potential energy of a cluster is partitioned into two contributions as follows:

$$V=N_P E_0(1-E_{\text{strain}})+E_{\text{nnn}}, \tag{7}$$

where the first term corresponds to the nearest-neighbors interaction. N_P is the number of nearest-neighbors pairs, E_0 the potential energy of the molecular dimer in its most stable configuration, and E_{nnn} is the contribution from the nonnearest neighbors. The strain energy is computed as follows:

TABLE III. Computed E_{strain} for several $(X)_{13}$ clusters. N_c is the crossover point (obtained from experiments and/or computer simulations).

$(X)_{13}$ cluster	E_{strain}	N_c
Ar	0.022	1000–2000[a,b]
N_2	0.095	~200[c]
CO_2	0.32	25–32[d]
SF_6	0.365	13–19[e]

[a]Reference 1.
[b]Reference 2.
[c]Reference 4.
[d]Reference 7.
[e]Reference 5.

$$E_{\text{strain}} = 1 - \left(\frac{1}{2N_P} \sum_{i=1}^{N} \sum_{j=1}^{N_i} \frac{E_{ij}}{E_0} \right), \tag{8}$$

where E_{ij} is the interaction energy between molecules i and j and N_i is the number of nearest neighbors of the molecule i.

The dominant term in Eq. (7) is the nearest-neighbor interaction (for 13 particles clusters, the contribution from non-nearest-neighbors interaction is less than 10% to the total energy). Thus two terms in the nearest-neighbors interaction are in competition. The lowest energy minimum for small rare gas clusters is icosahedral because it maximizes the number of nearest-neighbor contacts. However the inherent strain energy of the icosahedral morphology increases with increasing size and for shorter range potentials.[21,22] Hence, as either the size increases or the range decreases, the structure of the global minimum changes from icosahedral to cubic. In a recent work, Doye and Wales[41] have shown that, for this reason of short-range potential, model $(C_{60})_N$ clusters with $N>13$ presumably exhibit decahedral and close-packed structures, rather than icosahedral.

In a previous study, Wales has considered the effect of the anisotropic three-body interaction on the size dependence of the structure of atomic clusters.[42] It was shown that increasing anisotropy tends to favor the close-packing scheme and consequently lower the icosahedral to cubic crossover point (N_c).

Interaction between molecules is characterized by a strong anisotropy of the potential function. First of all the *repulsive* part of the potential is anisotropic and this leads to a shorter-range effect than the three-body dispersion terms. In addition, polyatomic molecules exhibit multipole moments and this also leads to an anisotropic Coulombic intermolecular interaction term. Thus it can be expected that, for a given cluster size, polyatomic molecular systems in the icosahedral morphology are more highly strained than their atomic clusters counterparts.

We have calculated the strain energy of model $(X)_{13}$ clusters (X=Ar, N_2, CO_2, and SF_6) in the global minimum of their potential energy surface. Our simulations (Table III) confirm that the more highly strained systems correspond to the lower N_c values (CO_2 and SF_6).

A direct comparison is possible between Ar, N_2, and CO_2 since they exhibit close-packed bulk structures. As no simple, straightforward relation exists between the strain energy and N_c for small clusters, we assume here that E_{strain} is roughly proportional to the inverse of the crossover point. We have then estimated the crossover point for N_2 clusters, and found $N_c = 100 \pm 50$. This is consistent with the experimental findings.[4] A computer simulation study is planned in order to check this prediction.

TABLE IV. Computed E_{strain}: (a) model $(N_2)_{13}$ cluster with a molecular quadrupole moment increased by a factor of 1.5 and 2; (b) model $(N_2)_{13}$ cluster with an internuclear bond length increased by a factor of 1.5 and 2.

(a) $Q_{\text{N-N}}/Q_{\text{N}_2}$	E_{strain}
1	0.095
1.5	0.201
2	0.305

(b) $l_{\text{N-N}}/l_{\text{N}_2}$	E_{strain}
1	0.095
1.5	0.212
2	0.294

As mentioned above, the interaction between carbon dioxide molecules are more anisotropic than between nitrogen molecules for both steric and coulombic reasons. Both effects are responsible for the increase in strain energy when going from $(N_2)_{13}$ to $(CO_2)_{13}$ clusters. This was shown (Table IV) by computing the strain energy for two model nitrogen systems in which either the quadrupole moment or the bond length were increased by a factor of 2.

Finally Wales *et al.*[43] has noticed that the ratios of the critical to the triple point temperatures of the four substances listed in Table III are 1.8, 2.0, 1.4, and 1.4, respectively, and appear to correlate quite well with the strain energies. This suggests that the energetic analysis recently developed by this author for atomic liquids might be useful in the structural analysis of molecular liquids.[44]

V. CONCLUSION

The strong differences in behavior between argon, nitrogen, carbon dioxide, and sulfur hexafluoride clusters can be understood by characterizing the structural, dynamic, and thermodynamic changes in terms of the underlying potential energy surface (PES) of the system.

A given small cluster of a given size may exhibit a phase transition whenever an energy gap is observed in the PES. In the case of melting, the phase transition is relatively sharp and is accompanied by a dynamical coexistence phenomenon. Two gaps in the PES have been observed in the case of $(N_2)_{13}$. The additional gap corresponds to an orientational phase transition which is presumably the finite size analog of the bulk rigid to plastic phase transition. On the other hand, small cluster may melt progressively without exhibiting any phase transition. This is the case for SF_6 clusters, for instance, in which no energy gap was found in the PES.

Understanding the difference in crossover point from icosahedral to bulk properties between different systems has long been a challenge to clusters physicists. The relevant

parameter could well be the inherent strain energy of the icosahedral morphology. Wales and co-workers have shown that this strain energy increases with size and for shorter range potentials.[21,22] Hence, as either the size increases or the range decreases, the structure of the global minimum changes from icosahedral to cubic. We show here that the strain energy increases with the anisotropy of the potential function, and that this explains the difference in crossover points between argon ($N_c \sim 1500$) and carbon dioxide ($N_c \sim 30$) clusters. A simple model leads to a prediction of $N_c \sim 200$ for nitrogen clusters.

In the second part of this work we shall describe the changes in structural, dynamics and thermodynamics of the carbon dioxide clusters in the size range ($N = 19-55$) in which the crossover from icosahedral to crystalline behaviour takes place. Examining the size dependency of the PES topography will make it possible to better understand how the bulk phase diagram emerges from the small clusters regime behavior in this particular case.

ACKNOWLEDGMENTS

D.J. Wales is gratefully acknowledged for fruitful correspondence. Fruitful discussions with G. Torchet, M. F. de Feraudy, and Ph. Millié are gratefully acknowledged.

[1] I. J. Farges, M.-F. de Feraudy, B. Raoult, and G. Torchet, J. Chem. Phys. **78**, 5067 (1983); **84**, 3491 (1986).
[2] S. Goyal, D. L. Schutt, and G. Scoles, J. Chem. Phys. **102**, 2302 (1995).
[3] L. S. Bartell and J. Chen, J. Phys. Chem. **96**, 8801 (1992); L. S. Bartell, *ibid.* **99**, 1080 (1995).
[4] G. Torchet and M-F. de Feraudy (unpublished).
[5] A. Boutin, J. B. Maillet, and A. H. Fuchs, J. Chem. Phys. **99**, 9944 (1993).
[6] A. Boutin, B. Rousseau, and A. H. Fuchs, Chem. Phys. Lett. **218**, 122 (1994).
[7] A. Boutin, A. H. Fuchs, M.-F. de Feraudy, and G. Torchet, J. Chem. Phys. **105**, 3671 (1996).
[8] X. Yang, E. R. Th. Kerstel, G. Scoles, R. J. Bemish, and R. E. Miller, J. Chem. Phys. **103**, 8828 (1995).
[9] T. L. Beck and R. S. Berry, J. Chem. Phys. **88**, 3910 (1987).
[10] D. J. Wales and R. S. Berry, J. Chem. Phys. **92**, 4283 (1990).
[11] J. Jellinek, T. L. Beck, and R. S. Berry, J. Chem. Phys. **84**, 2783 (1986); D. J. Wales and R. S. Berry, Phys. Rev. Lett. **73**, 2875 (1994); R. E. Kunz and R. S. Berry, Phys. Rev. E **49**, 1895 (1994); J. P. K. Doye and D. J. Wales, J. Chem. Phys. **102**, 9673 (1995).
[12] D. J. Wales and I. Ohmine, J. Chem. Phys. **98**, 7245 (1993).
[13] J-B. Maillet, A. Boutin, and A. H. Fuchs, Phys. Rev. Lett. **76**, 4336 (1996).
[14] B. W. van de Waal, Phys. Rev. Lett. **76**, 1083 (1996).
[15] D. J. Wales, Mol. Phys. **78**, 151 (1993).
[16] T. L. Beck, J. Jellinek, and R. S. Berry, J. Chem. Phys. **87**, 545 (1987).
[17] P. Labastie and R. L. Whetten, Phys. Rev. Lett. **65**, 1567 (1990).
[18] H. P. Cheng, X. Li, R. L. Whetten, and R. S. Berry, Phys. Rev. A **46**, 791 (1992).
[19] S. Weerasinghe and F. G. Amar, J. Chem. Phys. **98**, 4967 (1993).
[20] N. Quirke, Mol. Simul. **1**, 207 (1988).
[21] J. P. K. Doye, D. J. Wales, and R. S. Berry, J. Chem. Phys. **103**, 4234 (1995).
[22] D. J. Wales, Science **271**, 925 (1996).
[23] C. S. Murthy, S. F. O'Shea, and I. R. McDonald, Mol. Phys. **50**, 531 (1983).
[24] G. Cardini, V. Schettino, and M. L. Klein, J. Chem. Phys. **90**, 4441 (1989).
[25] H.-J. Böhm and R. Ahlrichs, Mol. Phys. **55**, 1159 (1985).
[26] S. Nosé, J. Chem. Phys. **81**, 511 (1984); Mol. Phys. **52**, 255 (1984).
[27] H. L. Davis, J. Jellinek, and R. S. Berry, J. Chem. Phys. **86**, 6456 (1987).
[28] D. Beeman, J. Comput. Phys. **20**, 130 (1976).
[29] F. H. Stillinger and T. A. Weber, Phys. Rev. A **25**, 978 (1982).
[30] R. A. Laviolette and F. H. Stillinger, J. Chem. Phys. **83**, 4079 (1985).
[31] S. Weerasinghe and F. Amar (private communication).
[32] M. Bertolus, V. Brenner, Ph. Millié, and J-B. Maillet, Z. Phys. D **39**, 239 (1997).
[33] F. Calvo and P. Labastie, Chem. Phys. Lett. **247**, 395 (1995).
[34] M. Bixton and J. Jortner, J. Chem. Phys. **91**, 1631 (1989).
[35] J. B. Maillet, A. Boutin, and A. H. Fuchs, Mol. Simul. **19**, 285 (1997).
[36] R. S. Berry, J. Jellinek, and G. Natanson, Phys. Rev. A **30**, 919 (1984).
[37] J. D. Honeycutt and H. C. Anderson, J. Phys. Chem. **91**, 4950 (1987).
[38] R. D. Etters, K. Flurchick, R. Pan, and V. Chadrasekharan, J. Chem. Phys. **75**, 929 (1985).
[39] T. A. Scott, Phys. Rep., Phys. Lett. **27C**, 89 (1976).
[40] J. Jortner, in *Physics and Chemistry of Finite Systems: From Clusters to Crystals*, edited by P. Jena *et al.* (Kluwer, Dordrecht, 1992), Vol. I.
[41] J. P. K. Doye and D. J. Wales, Chem. Phys. Lett. **262**, 167 (1996).
[42] D. J. Wales, J. Chem. Soc., Faraday Trans. **86**, 3505 (1990).
[43] D. J. Wales and J. P. K. Doye (private communication).
[44] D. J. Wales and R. S. Berry, Phys. Rev. Lett. **73**, 2875 (1994).